We are IntechOpen, the world's leading publisher of Open Access books
Built by scientists, for scientists

6,900
Open access books available

185,000
International authors and editors

200M
Downloads

154
Countries delivered to

Our authors are among the

TOP 1%
most cited scientists

12.2%
Contributors from top 500 universities

BOOK CITATION INDEX
CLARIVATE ANALYTICS
INDEXED

WEB OF SCIENCE™

Selection of our books indexed in the Book Citation Index
in Web of Science™ Core Collection (BKCI)

Interested in publishing with us?
Contact book.department@intechopen.com

Numbers displayed above are based on latest data collected.
For more information visit www.intechopen.com

Dielectric Elastomers for Energy Harvesting

Gordon Thomson, Daniil Yurchenko and
Dimitri V. Val

Additional information is available at the end of the chapter

Abstract

Dielectric elastomers are a type of electroactive polymers that can be conveniently used as sensors, actuators or energy harvesters and the latter is the focus of this review. The relatively high number of publications devoted to dielectric elastomers in recent years is a direct reflection of their diversity, applicability as well as nontrivial electrical and mechanical properties. This chapter provides a review of fundamental mechanical and electrical properties of dielectric elastomers and up-to-date information regarding new developments of this technology and it's potential applications for energy harvesting from various vibration sources explored over the past decade.

Keywords: dielectric elastomer, circuits, materials, applications, electrostatic

1. Introduction

Energy harvesting (EH) is a process of converting energy existing in other forms or wasted energy into electrical energy that can be used as an alternative to the existing energy sources. Despite the semantics behind the words *harvesting* and *scavenging* the first one has been widely accepted in literature and will be used throughout this paper. EH from vibrations has formed its own niche because many natural phenomena as well as man-made machines and structures generate vibrations that can be converted into electrical energy. For instance, different methods can be used, various materials can be employed, and linear, parametric or nonlinear systems can be utilised for optimising the devices' efficiency. A number of transduction methods capable of such a conversion have been suggested, including piezoelectric, electromagnetic, electrostatic and triboelectric.
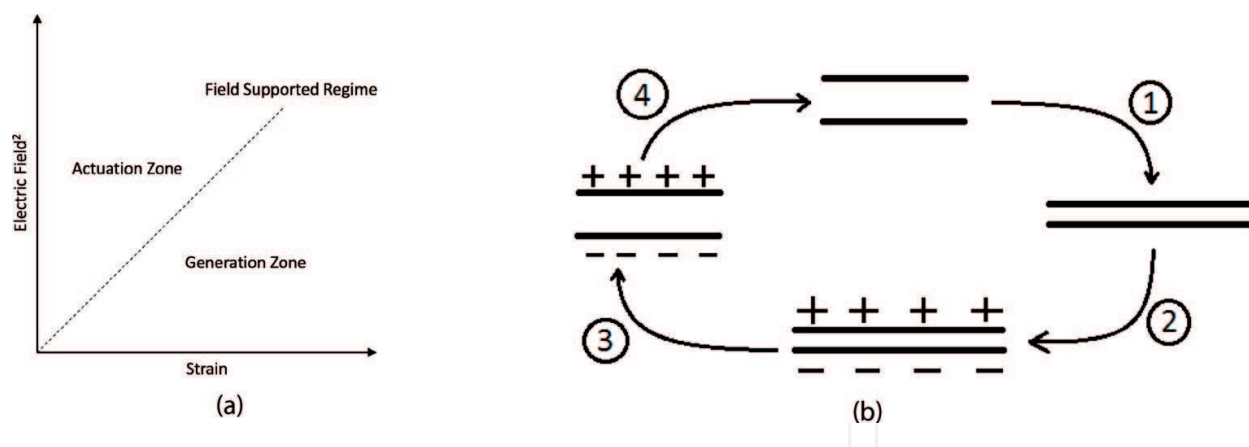
Figure 1. Basic principals of dielectric elastomer energy harvesting. (a) Actuation and generation zones. (b) The energy harvesting cycle for a dielectric elastomer.

EH using dielectric elastomeric materials is based on the principle of varying capacitance, however, instead of a traditional capacitor with two parallel plates separated by air a dielectric elastomer (DE) is used. This polymer, coated with compliant electrodes on each side, becomes a variable capacitance capacitor and can be used in two opposite modes: actuation, with a high potential in soft robotics and energy generation (**Figure 1(a)**). When the electric field is above its supported regime a DE is in the actuation zone, below—the generation one. Although there are many interesting and useful applications of DE actuators, this chapter will concentrate on the energy harvesting potential of DEs.

In the energy harvesting mode DEs can generate electricity when stretched by an externally applied force. The DE EH approach has recently seen an increasing amount of attention from a variety of science branches, including chemistry, electrical and mechanical engineering, robotics and MEMS, due to the multidisciplinary nature of the topic and a wide range of potential applications.

Pioneering work on DE EH was conducted by Pelrine et al. [1], who set the basic principles of using DEs for EH. Since then various advantages and disadvantages of this EH method have been investigated, in particular in the context of its high energy density [2]. The maximum energy density that has been achieved by a DE generator is $3.8 \mu W/\text{mm}^3$ [3], whereas the electromagnetic and piezoelectric generation resulted in $2.21 \mu W/\text{mm}^3$ [4] and $0.375 \mu W/\text{mm}^3$ [5] respectively.

This chapter focuses on the DE EH applications and provides an overview of the work done up-to-date in the field, mainly after the book published in 2008 [6]. The chapter is divided into five sections based on the main components of the DE EH theory and cover electrical and material background, failure modes, initial voltage issue and applications.

2. Electrical background

The basic equation describing the behaviour of an ideal capacitor, with two parallel plates and air between them, is well-known and states that:

$$Q = CV, \quad C = \frac{\epsilon\epsilon_0 A}{z} \tag{1}$$

where Q is the charge held on the electrodes, V is the voltage over the capacitor and C is the capacitance, ϵ is the relative permittivity of the substance between the plates, $\epsilon_0 = 8.854 \times 10^{-12}\,\mathrm{Fm}^{-1}$ is the permittivity of free space, A represents the effective area of the plates and z is the distance between the plates. When the distance between the plates is changed (the plates area is assumed to be a constant) the capacitance will be changed accordingly. Thus, the variable capacitance indicates the two energy harvesting schemes: constant voltage and constant charge. First one assumes the application of an initial voltage to the plates and then the distance between the two plates is reduced, leading to an increase in the capacitance and thereby in the charge increase that can be harvested at the minimum distance between two plates. A similar approach can be employed when the constant charge scheme is used. In this case increasing the distance between the two plates reduces the capacitance and thereby increases the voltage that can be harvested. The energy gain is related to the difference in its values between the maximum and minimum capacitances. The electrical energy stored in a classical capacitor is given by the following equation:

$$U = \frac{1}{2}CV^2 = \frac{1}{2}QV \tag{2}$$

where the second equality can be obtained by using Eq. (1). However, in some applications moving physically capacitor plates is not feasible or efficient. Thus, a material mimicking the properties of a capacitor can be used instead and DEs are a perfect fit for that. Indeed, DEs are extremely poor conductors, relatively inexpensive in production and can be repeatedly deformed and stretched. To manufacture a DE-based capacitor a DE is sandwiched between two deformable electrodes serving as an insulator. Another important property of DEs from the EH point of view is their high deformability because it enables the capacitor to reach high values of the capacitance by stretching the DE and, subsequently, significantly reducing its thickness, i.e. z, as can be seen from Eq. (1) expressed in a slightly different form:

$$C = \frac{\epsilon_d \epsilon_0 A}{z} = \frac{\epsilon_d \epsilon_0 P}{z^2} \tag{3}$$

where $P = Az$ is the material volume and ε_d is the relative permittivity of the dielectric elastomer. It should be noted that whilst the area of the electrodes (plates) for a conventional electrostatic energy harvester remains constant, the area of the DE capacitor changes under deformation. Since a DE can usually be treated as an incompressible material, i.e. its volume does not change under deformation, Eq. (1) can be expressed in the form of Eq. (3). Thus, cyclic stretching can be used to increase an initial bias voltage of the capacitor to a higher voltage that can be harvested. The diagram demonstrating all stages of this repeatable EH process is presented in **Figure 1(b)**, where the numbers 1–4 in **Figure 1(b)** represent the stages of the energy harvesting cycle and may be explained as following:

1. The DE is stretched increasing the area of the electrodes and decreasing the thickness between the electrodes, leading to an increase in the capacitance.

2. A charge is placed over the DE.

3. The DE is allowed to return to its original shape that decreases the capacitance, resulting in a higher potential voltage over the elastomer.

4. The gained electrical energy is then removed.

Pelrine et al. [1] derived the following formula for estimating the energy gain per cycle, e_g:

$$e_g = \frac{P\epsilon_d\epsilon_0}{2}\left(E_c^{\ 2} - E_s^{\ 2}\right) \tag{4}$$

where E_c and E_s, defined as $E = V/z$, represent the electric field at the contracted and stretched states, respectively.

Having outlined the basic principle of energy harvesting using DEs, let us consider electrical methodology designed for EH. Currently, three EH schemes are being used: constant voltage, constant charge and constant field. The term 'constant' refers to the electrical state of the DE during the transition of the material from the stretched to its relaxed state. The first two schemes are the most investigated ones and have been used before in electrostatic EH; their advantages and disadvantages have been discussed in [7, 8]. The cycles' stages for constant voltage and constant charge are shown in **Figure 2(a)** and **(b)**, where λ_{min} and λ_{max} denote the minimum and maximum stretching states, respectively.

The constant voltage scheme in **Figure 2(a)** begins with stretching the DE and charging it at its maximum stretching state (line 1). Reaching the maximum voltage, controlled by the electrical breakdown (Section 5), the material is released and returns to its unstretched state along the constant voltage line 2 with the corresponding decrease in the capacitance. To maintain the constant voltage the charge needs to be decreased from Q_{high} to Q_{low}; the charge difference flows to a reservoir (e.g. battery) through the circuit controlled by diodes. The capacitor is then discharged into the reservoir so that the DE returns to its original state (line 3), and after that the next cycle can begin. The amount of harvested energy per one cycle is represented by the area circumscribed by the three lines and can be calculated as [8]:
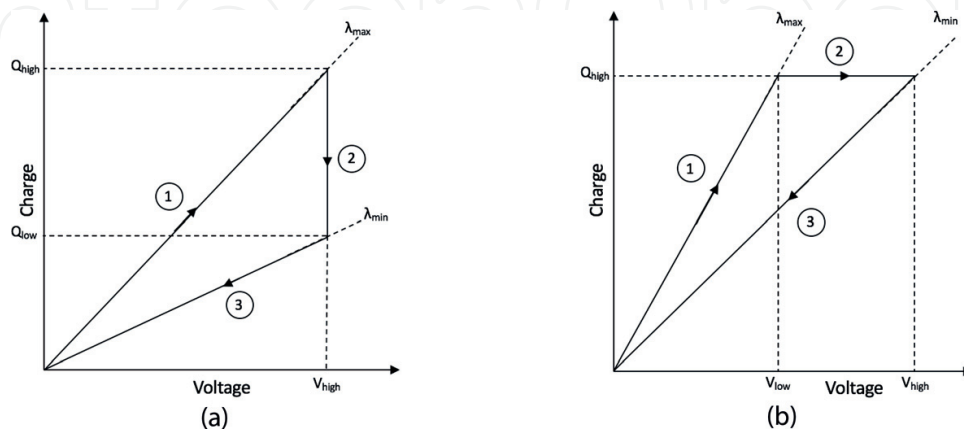

Figure 2. Common energy harvesting schemes. (a) Constant voltage scheme. (b) Constant charge scheme.

$$e_g^V = \frac{1}{2}\Delta C V_{high}^2 \tag{5}$$

where ΔC is the difference between high and low capacitance values.

A range of electrical circuits for DE generators is discussed in [7]. In particular, it is mentioned that the constant voltage scheme is the most practical one to realise. This is due to the lack of switches that can be difficult to effectively integrate into a EH device, especially considering the exact timings necessary to achieve the maximum efficiency.

The constant charge scheme is depicted in **Figure 2(b)** and uses the variable capacitor as a pump to move a charge from a low to high voltage. This is done by initially stretching the DE and placing a charge onto it while the latter is at its high stretching state (line 1). The power supply is then disconnected and the DE is released to return to its original state increasing the voltage from V_{low} to V_{high} due to the decreasing capacitance (line 2). At this point the electrical energy is harvested and the DE reverts back to its initial state (line 3). The energy harvested per one cycle is represented by the area enclosed by the three lines and equals [8]:

$$e_g^Q = \frac{1}{2}\Delta C V_{low} V_{high} \tag{6}$$

Although the constant charge scheme may be useful and effective as shown by Blokhina et al. [9], who considered a constant charge circuit for a nonlinear electrostatic vibration energy harvester, it is hampered by its need for switches which can reduce the power output and increase the complexity of the entire circuit. Thus, following this argument and discussion in [7] it is save to say that the constant voltage scheme is more preferable for implementation. However, high voltage is not suitable for most micro-power devices operating at a low voltage, in which a DC-DC voltage step down is normally needed. This extra component can reduce the overall efficiency of the DE EH so that the constant charge scheme may provide a greater efficiency for such applications.

Most recent works have been based on the electrical circuitry first implemented by Huang et al. [10], which operates according to the constant voltage scheme. In the latter work the authors devised an electrical circuit, shown in **Figure 3(a)**, which can measure the charging and harvesting currents as well as the voltage over the DE. It has also been confirmed that
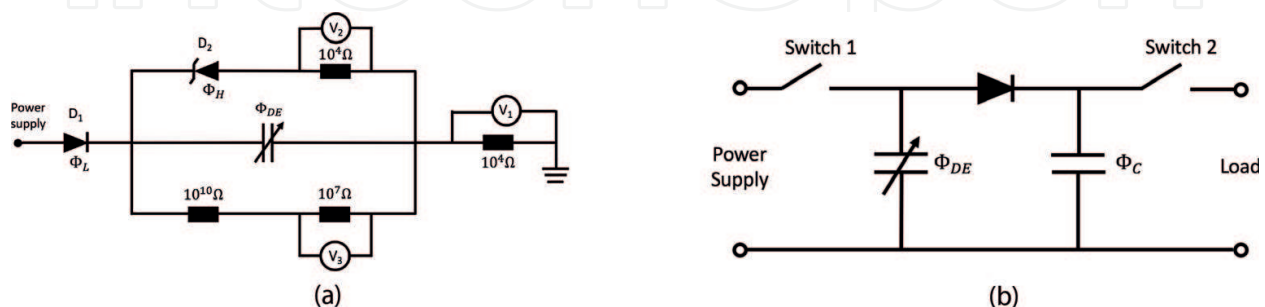

Figure 3. Dielectric elastomer energy harvesting circuits. (a) A common circuit for dielectric elastomer EH research. (b) A circuit highlighting features for the optimised scheme.

there is a proportional quadratic dependence of the dielectric capacitance on the membrane stretch. Using this result it was found that the dielectric constant of the common DE VHB 4905 (3M) was $\epsilon = 4.03 \pm 0.17$.

The circuit shown in **Figure 3(a)** works as following. The DE is charged using a power supply; the charge passes through a rectifier diode, D_1, at the maximum stretch of the DE. As the DE stretch reduces, the voltage initially increases at a constant charge, with no new charges flowing through D_1. This continues until the voltage over the DE reaches a pre-determined discharge voltage, governed by the Zener diode D_2. Once this voltage has been reached, the charge leaves the circuit through this diode. Finally, the membrane is stretched out again, lowering the voltage of the charge that remains, until the voltage reaches that of the power supply, which is connected again and the cycle is repeated. The circuit shown in **Figure 3(a)** is very useful for DE EH research since through its various components a large amount of information can be gathered about the behaviour of the DE generator. For example, using the lower of the three parallel branches, which behaves as a voltage divider, the voltage over the DE can be constantly monitored using V_3. Similarly, V_1 and V_2 can be used to measure the charging and harvesting currents, respectively, utilising the measured voltage in each voltmeter and the known resistances. Once these currents are known the input and harvesting charges can be found using $Q = \int idt$. The net energy gain can then be estimated as $\Delta E = (V_{high} - V_{low})\Delta Q$.

The above discussion is related to the ideal material behaviour with no failure modes considered and no losses taken into account. Electromechanical coupling, e.g. further stretching of a DE when a charge is applied and the corresponding change of the capacitance, has also not been mentioned. Since DEs may experience electrical and mechanical failures (Section 4) it is essential to account for them [2]. These failure modes, shown as curves on the $Q - V$ plane in **Figure 4(a)**, change the idealistic EH picture. Apparently, the maximum harvested energy corresponds to the maximum area enclosed by the lines connecting the maximum and minimum stretch states, without crossing to the failure regions. In **Figure 4(a)** such a cycle is constrained between the aforementioned upper and lower stretch states. It is also limited by two failure modes, dielectric breakdown (DB) and electromechanical instability (EMI), which are discussed in Section 4 in greater detail. An 'optimal' scheme, developed by Shian et al. [11], built upon the conventional EH schemes as shown in **Figure 4(a)**. In [11] the authors proposed
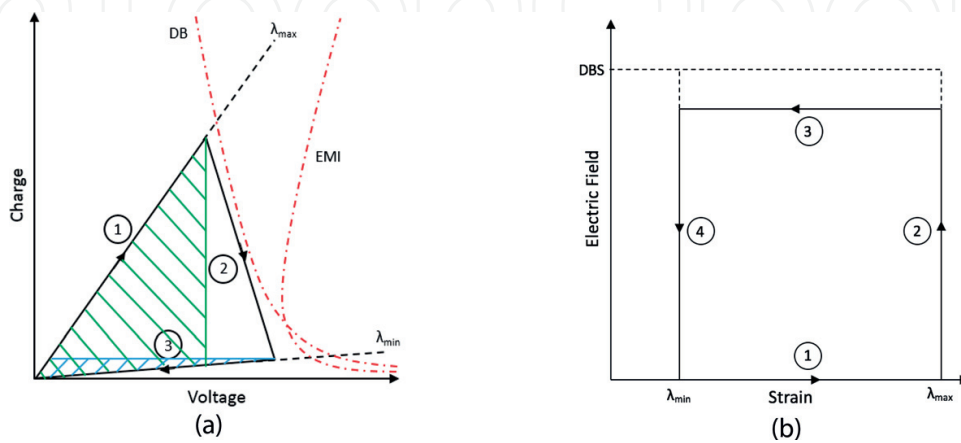

Figure 4. More recent energy harvesting schemes. (a) The optimised scheme. (b) Constant field scheme.

this new harvesting cycle, which utilises the circuit diagram shown in **Figure 3(b)**. This scheme maximises the working area within the limits imposed by the failure criteria set out in [2]. The optimal cycle is shown in **Figure 4(a)** in black, whereas the areas for the constant voltage (green) and constant charge (blue) are also superimposed into the graphs to demonstrate the difference between the schemes. One can see clearly the benefits of the optimisation by simply comparing the corresponding areas. Following one of the conventional methods (constant voltage or charge) a designer must lose large sections of the available energy in order to avoid failure. It should be noted that the values for the stretch during the cycle and the maximum charge or voltage used in the conventional schemes can be used to alter their respective areas on **Figure 4(a)**, in accordance with Eqs. (5) and (6). However, this system is hard to implement for a real DE material as its rate of the stretch decrease will not be as ideal as indicated in [12]. In that work the authors attempted to optimise the system of harvesting by showing an analytical method of determining the ideal stretch ratio at which the membrane discharging should occur. Additionally, Hoffstadt et al. [13] conducted an optimisation of the conventional EH cycles and determined the ideal charging and discharging times for maximal energy gain in the optimised scheme.

The circuit, presented in **Figure 3(b)** was proposed to work with the above EH scheme. The first phase of this cycle is charging the DE at its maximum stretch state, after which switch 1 is used to disconnect the DE from the supply. The second phase of the cycle is decreasing the DE stretching. This sees the DE discharge into a temporary storage capacitor, Φ_C, which is connected in parallel to the DE and the harvesting section of the circuit. This discharging to the capacitor will cause the charges on the actual DE to drop, however the voltage will continue to increase as shown by Eq. (3). The final stage of this cycle occurs at the low stretch state, where all electrical energy is removed from both the DE and the temporary capacitor.

A relatively new constant field EH scheme, shown in **Figure 4(b)**, proposed to improve the conventional schemes. This cycle begins with initial stretching of the DE to its maximum level (line 1). The DE is then charged up to an electric field pre-determined by the designer (line 2). After that the DE streching is reduced back to its original level at a constant electric field (line 3). It is worth to recall that the electric field is defined as $E = V/z$, therefore, at constant electric field a decrease in the DE stretching and the corresponding increase in the DE thickness lead to an increase in the voltage over the DE. This is an advantage over the constant charge scheme, since at the latter the electric field increases during the reduction of DE stretching that may cause failure due to dielectric breakdown (Section 4). The final stage of the circuit is to remove the electrical energy from the DE, returning the latter to its original state (line 4). Since failure by dielectric breakdown is of no concern for this scheme this allows the DE to be operated closer to its dielectric breakdown strength (Section 4). Czech et al. [14] analytically compared the ideal constant voltage, constant charge and constant electric field schemes and found that the constant electric field was the most effective. However, it should be noted that maximising the energy output by increasing the electric field may have an adverse effect on the lifespan of the generator [15].

A few other works have been recently done on improving electrical aspects of DE EH, e.g. Kaltseis et al. [16] developed an experiment based on operating a DE generator between two charged reservoirs of different voltages that allowed them to monitor separately electrical and mechanical energies and determine the net energy gain.

3. Material background

DEs belong to a group of electroactive polymers (EAP) that received this name because of their ability of changing their shape under applied electrical field. Essential properties of DEs for EH applications are low mechanical stiffness, high dielectric constant, high electrical breakdown strength, high elastic energy density and high deformability. There are a number of DEs possessing these properties including acrylates (e.g. VHB 4905 and 4910), silicones, polyurethanes, rubbers, etc. It is also worth to note that DEs have a number of properties such as nonlinear stress-strain relationship, viscoelasticity (i.e. time-dependent behaviour), electromechanical coupling, temperature-dependent performance, etc., which significantly complicate the modelling and design of DE generators. Quite extensive overview of the main properties of these materials in the context of EH can be found in [17–21]. The relevant material properties of DEs and their modelling are also briefly considered further in this section.

3.1. Material properties

A typical DE-based system (i.e. capacitor) comprises a DE membrane sandwiched between two electrodes, as depicted in **Figure 5**. Depending on the purpose of the system in-plane stretching of the DE can be done either by applying an electrical field (actuator) or mechanical deformation (harvester). The applied electrical field causes the so-called Maxwell stress in the material due to the interaction of opposite charges on both electrodes, resulting in the DE stretching. This concept has been well demonstrated, e.g. by Mockensturm et al. [22] who manipulated a DE membrane by altering the applied electric field to move the membrane between its various steady state equilibria. Tensile stresses in the plane of the DE membrane, caused by in-plane or out-of-plane loading, lead to the material deformation reducing the membrane thickness and increasing its area, thereby changing the capacitance of the DE-based capacitor.

A well-known material property of DEs is their high deformability, i.e. the ability to undergo large deformations without rupture. The stretch ratio (or simply stretch), defined as a ratio of the stretched length to the initial one $\lambda = L_s/L$, may reach for some materials up to 900% [23, 24]. This property is very important since it enables to impose relatively high levels of
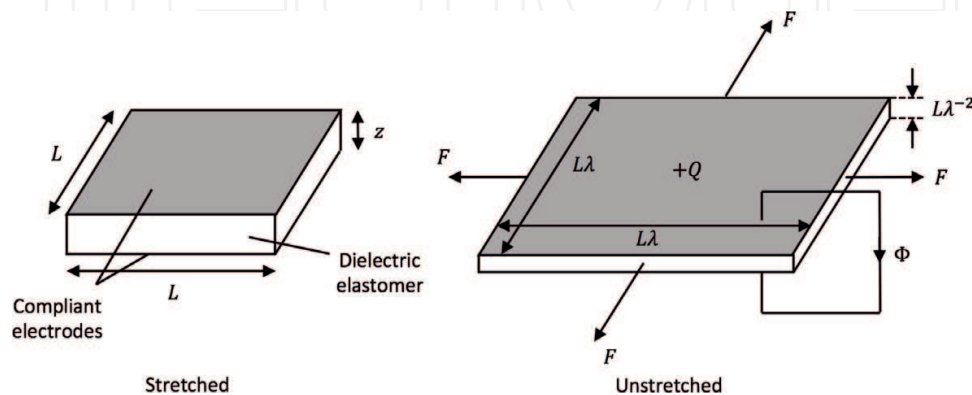

Figure 5. Loading of a dielectric elastomer.

pre-stretch on DE membranes that improves their material performance, in particular increases the dielectric (i.e. electrical breakdown) strength and reduces the effective compressive modulus [25]. At low deformations the material demonstrates strain softening that changes to stiffening at higher deformations. This type of mechanical behaviour is usually described by a hyperelastic constitutive model under the assumption that the DE is an ideally elastic material. Different hyperelastic models used for DEs will be briefly described in the next sub-section. To determine parameters of such models data from uniaxial tensile tests, and for more accurate determination also from biaxial tests, are needed. Results of uniaxial and biaxial tests of VHB 4910 were reported in [26, 23] and for silicone-based elastomers in [27]. Results of uniaxial tests of natural rubbers can be found in [28].

Another important property that significantly affects the mechanical behaviour of DEs is viscoelasticity, which occurs due to the realignment of polymer chains of the materials under loading and leads to time-dependence of deformations and stresses. For example, stress-stretch (or strain) curves of DEs depend on the strain (i.e. loading) rate and are usually show stiffening with increase in the rate, e.g. [24]. In particular, viscoelasticity causes dissipation, i.e. losses, of the mechanical energy that, in its turn, reduces the efficiency of DE generators [10, 29–31]. The losses are associated with a hysteretic behaviour of a DE, i.e. the stress-stretch curves of the material follow different paths during loading-unloading forming a hysteresis loop whose area represents the energy loss, e.g. [32]. Creep and stress relaxation are other phenomena associated with viscoelasticity. Creep is usually defined as a time-dependent increase in deformation under constant load, while stress relaxation is a decrease in stress under constant deformation. Creep is more important for DE actuators, while stress relaxation may have a significance influence on the performance of both DE generators and actuators. Typical tests to determine viscoelastic characteristics of a DE as well as parameters of a model describing the material's viscoelastic behaviour include loading-unloading tests at a range of strain rates, single-step relaxation tests at various stretch levels and multi-step relaxation tests, in which at each step loading follows by a sufficiently long holding period to allow for stress relaxation [32]. The tests are usually uniaxial, however, equi-biaxial tests may also be useful. Most of the experimental studies on the viscoelastic behaviour of DEs have been carried out for VHB 4905 and VHB 4910 [24, 26, 32–36]. In particular, it has been shown that for this material very rapid stress relaxation occurs within the first few seconds of holding, while after 30 min the remaining stress almost stabilises [32]. Past experiments also showed that for VHB polymers the viscoelastic relaxation time is of the order of 10^2 seconds at room temperature [37]. Pharr et al. [24] demonstrated that the strain rate and the specimen size had a noticeable influence on rupture of VHB 4905. Hossain et al. [33] reported results of relaxation tests under both mechanical and electric loading and showed that the latter had a major effect on the time-dependent behaviour of VHB 4910. A few results of similar experiments for other DEs have been published. In particular, Schmidt et al. [23] presented results of uniaxial and equi-biaxial relaxation tests for Interpenetrating Polymer Network Reinforced Acrylic Elastomers (IPN), which were produced on the basis of VHB 4910. Bernardi et al. [27] published similar results for silicone-based DEs.

A hysteretic behaviour of DEs, especially of rubbers and rubber-like materials, and associated with it loss of mechanical energy can also be due to the so-called Mullins effect, also known as

stress softening [38]. This effect causes a decay of the elastic stiffness of a material under repeated loading-unloading, which depends on the maximum stretch previously experienced by the material. Recommendations regarding experimental characterisation of the effect can be found in [39].

Effects of the operating temperature on the material properties of VHB 4910 and the performance of a generator made of this material were investigated by Chen et al. [40]. In particular, it was found that the generator operated more efficiently under lower temperatures due to smaller viscoelastic losses.

As can be seen from above, so far VHB 4905/10 (3M™) have received most attention from researchers. However, other DEs, in particular natural rubbers and polyurethanes (PUR), have been also investigated and demonstrated good potential for EH, in some cases better than VHB, e.g. [28, 41, 42]. One of the researches, [41], examined the influence of stretching on the electrical properties, such as the electrical (or dielectric) breakdown strength (DBS) and dielectric constant, of VHB 4910 and natural rubber and suggested that the latter had advantages over VHB in the context of EH. It also necessary to note that in our overview of the DE material properties we mainly concentrated on their mechanical properties, while the electrical properties were only mentioned in relation to the last referred publication. Of course, the electrical properties of DEs are also very important for EH and were considered in a number of the references provided above. Detailed recommendations on experiments that can be used to determine both mechanical and electrical properties of DEs are given in [39].

Finally, based on data presented in [43] we include **Table 1**, which provides the important mechanical and electrical properties of some DEs that can be used for EH. More information about specific DEs appearing in the table, in particular polyurethanes (i.e. PUR 1, PUR 2, etc.), can be found in the source [43]; acrylate means VHB 4905.

3.2. Modelling

Modelling is essential for the development and design of DE-based devices for EH. The idea is to simulate the performance of such devices using analytical and/or numerical models and reduce the need for time-consuming and relatively expensive experiments. Basic theory of DEs

Name	Mechanical properties				Electrical properties	
	DE thickness (μm)	Break Strain (%)	E at 50% (MPa)	Creep (30 min) (10% Def.)	ε_d (1/8 Hz)	DBS (MV/m)
PUR 1	50	421	3.36	24	6	218
PUR 2	50	252	1.47	2.9	7.1	108
PUR 3-1	49	251	1.96	1.9	7.1	132
PUR 3-2	97	319	1.3	6.5	8.0	102
Silicone	45	422	0.25	16	2.5	80
Acrylate	498	879	0.04	70	4.5	31

Table 1. Comparison of various elastomer properties.

based on thermodynamics and continuum mechanics was described in [44]. In this section we overview some specifics of its practical implementation.

As has been noted previously, the elastic behaviour of DEs under large finite deformations is usually modelled within the hyperelasticity framework. This means that the material is assumed to be ideally elastic and that stress-strain (or stretch) relationships are obtained based on a strain energy density function, which is expressed as a function of the invariants of the Cauchy-Green deformation tensor, e.g. [45]. Thus, a particular hyperelastic constitutive model fully depends on the corresponding formulation of the strain energy density function. So far various formations of the strain energy density function and, subsequently, hyperelastic models have been used to describe the elastic behaviour of DEs under large deformations, e.g. Neo-Hookean [46–48], Mooney-Rivlin [49], Ogden [27, 49, 50], Yeoh [51], Arruda-Boyce [26, 52] and Gent [48, 53, 54]. Of course, this list is far from being exhaustive. There are other hyperelastic models that could also be used for modelling the constitutive behaviour of DEs. Many researchers have compared the predictions provided by different hyperelastic models with the experimentally observed behaviour of DE membranes, e.g. Yeoh, Ogden and Arruda-Boyce [26], Mooney-Rivlin and Ogden [55], Neo-Hookean and Gent [48]. It is important to note there is no universal hyperelastic model that would provide accurate and reliable predictions for all DEs. A hyperelastic model that yields excellent results for a particular DE under specific conditions may be inapplicable for another DE. An extensive review of the hyperelastic models can be found in [56, 57].

The hyperelastic models describe the time-invariant behaviour of DEs. However, this is not the case because of viscoelasticity. Thus, in order to achieve more realistic predictions of the DE performance under mechanical and/or electrical loading, especially cyclic or dynamic loading, the time-dependency due to viscoelasticity needs to be taken into account. Wissler and Mazza [51] suggested to use the quasi-linear viscoelastic (QLV) model. This model is based on the assumption that the relaxation function is independent of the stretch ratio (or strain), i.e. depends only on time. The relaxation function was determined based on experimental results using the so-called Prony series. To combine the hyperelastic and QLV models, the coefficients of the energy density function are multiplied by the relaxation function. The same approach was also used by Wang et al. [58]. The model provides reasonable for quasi-static creep and stress relaxation problems; however, its predictions noticeably deviated from experimental results in the case of dynamic loading as the number of cycles increased [26].

Many researchers use models based on classical rheological models such as Maxwell and Kelvin-Voight with added elements. One of the most popular models is the so-called standard linear solid model presents a Maxwell element in parallel with an elastic spring, e.g. [37, 59, 60]. Others used an extended Kelvin-Voight model, i.e. a Kelvin-Voight element in series with an elastic spring [58, 61]. A model combining in parallel Maxwell and Kelvin-Voight elements has also been suggested [62]. Models based on the generalised Maxwell model, also known as Maxwell-Wiechert model, have also been proposed and implemented [56, 63, 64]. An extensive review of viscoelastic models can be found in [65].

It is worth to note that the viscoelastic models described above were usually implemented for uniaxial or equi-biaxial problems that led to a set of ordinary differential equations, which were solved numerically. However, to solve more general problems or obtain more accurate

results (i.e. avoid simplifying assumptions) the finite element (FE) modelling is needed. One of the main challenges here is to develop and implement finite elements that take into account electromechanical coupling since commercial FE software, e.g. ABAQUS, does not currently provide such an option. FE models for simulating the DE behaviour under both mechanical and electrical loads have been proposed in [66–68]. In particular, Henann et al. [67] employed the developed FE model to carry out an analysis of both DE actuator and generator. Jean-Mistral et al. [69] also used FE modelling to investigate a new technique for DE EH.

4. Failure modes

In order to fully asses the DE generators potential the failure mechanisms have to be considered. In general there are two types of failures a DE device may face: material and manufacturing related. Whereas the former are discussed in this section the latter are not because they are mostly related to imperfections due to the manufacturing process. This group includes but not limited to failures due to non-uniform stretching of the material over the working area, poor or uneven distribution of charges (electrodes) over the working surface, loss of contact between electrodes and working surfaces, others malfunctioning of electrodes during normal operation. The material related failures may be combined into four groups: rupture by stretch, loss of tension, electrical breakdown and electromechanical instability.

Rupture by stretching occurs when the membrane is stretched too much and the internal strain becomes too high leading to the material ripping, as explained by the classical stress-strain curve for a material. Loss of tension occurs when the initial voltage placed over the membrane is enough to remove the pre-strain put onto the generator in its construction.

Dielectric breakdown is a complex topic, however it is enough to say that there is a specific electric field at which the membrane will essentially become a conductor and the generator will fail. As the electric field is given by $E = V/z$, the dielectric breakdown strength (DBS) is inversely proportional to the thickness, thus the thinner the material the larger its DBS [70]. This was investigated further by Tröls et al. [41] who reported how the dielectric breakdown strength and dielectric constant is influenced by the stretch of the material. Their main findings regarding E_{EB} and ϵ for 3M[TM] VHB 4910 are shown in **Table 2**. Pre-straining, typically performed during the manufacturing stage, can improve the DBS. The pre-straining is done by taking the DE to a minimum level of stretch λ_{min} in a device. Besides improving the DBS of the material, pre-straining negates the risk of failure by loss of tension. The increase in DBS of VHB 4910 (3M[TM]) by 1100% under an equal biaxial pre-straining of 500% has also been reported in [71].

Value	$\lambda = 1$	$\lambda = 2$	$\lambda = 3$	$\lambda = 4$	$\lambda = 5$
E_{EB} Vμm^{-1}	–	100	124	145	163
ϵ (1 Hz)	4.24	–	3.83	–	3.44

Table 2. Dependence of the electrical properties of VHB 4910 on the stretch ratio.

Electromechanical instability occurs due to nonlinearities in the materials behaviour. As the membrane stretches due to increasing electrostatic forces, nonlinearities occur in the stretching and some areas will become wrinkled producing thinner and thicker sections.

The failure modes associated with dielectric elastomers were investigated by Koh et al. [2] who derived the equations of failure for the two work conjugate planes of force-displacement and voltage-charge. These equations can then be plotted as lines on the respective graphs with the enclosed area representing the maximum working area, which can be used to find the maximum energy per cycle for a specific membrane. This work showed that for a membrane with modulus, $\mu = 10^6 \mathrm{N/m}^2$, permittivity of $\epsilon = 3.54 \times 10^{-11} \mathrm{F/m}$ and density of $\rho = 1000 \mathrm{kg/m}^3$, an energy gain of 6.3 J/g per cycle was achieved. However, this would be difficult to implement in experimental conditions. Pelrine and Kornbluh [72] then updated this describing the fundamental science and derivations behind dielectric elastomers as well as covering the failure methods and a variety of dielectric elastomer configurations. In addition to the commonly cited failure limits set out by Koh et al. [2], Zhou et al. [73] conducted an investigation into the performance and lifetime of dielectric elastomer generators subjected to a cyclic deformation. Their work hypothesised that a decrease in the generator output is due to fatigue cracks forming on the membrane. In order to minimise this effect a smaller strain and deformation rate is proposed to increase the lifetime of the device. With an increase in applied voltage keeping the output energy higher, in accordance with Eq. (4).

Other failures that have not been mentioned above may be associated with the loss of electrical contacts, different stretching capabilities of the DEs and electrodes, fatigue and durability, as well as multiscale instabilities [74, 75].

5. Initial voltage issue

One of main concerns with dielectric elastomer generators (DEGs) is the need for an initial voltage. Given that the larger the supply voltage, the larger the energy gain, ideally the supply would be in the kilovolt range, which causes an issue for small-scale or portable generators. One solution to this problem is self-priming circuits proposed by McKay et al. [76]. This circuit allows any energy not used in powering the load to go back into the energy supply, so that over time this increases the power input to the system. In their experiment the input voltage was taken from an initial 10 V to 3250 V after only 236 cycles. This work is the basis for many future real world applications, since a high voltage DC power supply or transformer is not commonly available at small-scale portable sizes. This work would allow generators to be started with low voltage batteries and power up to a working voltage. Illenberger et al. [77] further advanced the theoretical aspect of self-priming circuits by providing a mathematical analysis backed up by experimental validation with an accuracy of 0.1% after five cycles. Panigrahi and Mishra [78] built and simulated an electrical model of a dielectric elastomer generator using the common electrical simulation software, Pspice.

The use of self-priming circuits would allow other vibration energy harvesting techniques to be used to initialise a dielectric elastomer generator, which has been explored in some works

including [69]. Their work used electret technology to generate a bias voltage of 100 V which acted as the input to the DEG. In a later publication [79] this idea was studied by a finite element modelling. In general there is a great potential in combining some other types of energy generation with the self-priming circuit to raise the bias voltage to a level required.

6. Applications

A clear metric of progress being made in any energy generation field is evidenced in the new applications and performances of new devices. For that reason this section will highlight some of the significant breakthroughs made in recent years.

6.1. Indoor tests

Huang et al. [80] developed a DEG that was stretched radially, in-plane, in a laboratory setting. Their device had an energy density of 550 J/kg and an efficiency of 22.1%. McKay et al. [81] developed and tested a generator in laboratory conditions that consisted of 42 membranes placed on top of each other. The total volume of the device was 0.86 cm^3 and it could produce an output power of $300\,\mu W$ at an excitation frequency of 0.5 Hz. This design was further developed [3] using 48 membranes within the same volume and a larger applied voltage saw the output power increase to 1.8 mW at 1.6 Hz. Lai et al. [82] conducted a laboratory test on dielectric elastomers in the application of human walking. Their device was simple in nature and generated a relatively low energy gain, $10 - 50\,\mu J$, however it did experimentally prove the validity of energy harvesting from human walking. Kaltseis et al. [16] conducted a laboratory based experiment on a dielectric elastomer generator in diaphragm mode and showed a specific energy of 102 mJ/g and an average power of 17 mW/g, however it only achieved a 7.5% efficiency.

6.2. Wave energy converters

There are several types of wave energy converters that utilises DEs. Moretti et al. [83] proposed a generator called poly-surge that has to be sealed to the seabed. Their numerical study based on this design provided an output of 1.56 MW; however, this was based on 15 m^3 of dielectric elastomer and a model, which unrealistically assumed no losses due to viscoelasticity. Later Moretti et al. [84] developed a generator, similar in principle to an oscillating water column (OWC) generator, but using DEs instead of an air turbine. Their generator had an output of 0.3 J, or 173 J/kg, which is equivalent to 0.15 W. Vertechy et al. [85] have also investigated an OWC generator and experimentally tested it in a tank at a scale of 1:50. Their scaled model produced a maximum power of 76.8 mW. However, if the model was built at its full scale size, the authors estimated that it would be capable of producing 68 kW of power at the optimal wave conditions of 2 m height and a period of 11.7 s. Lv et al. [48] developed a DE-based wave energy converter for capturing heaving motion of waves. Their work showed that as the input voltage increased the experimental and theoretical power output both increased as expected,

but the efficiency dropped. This was mainly due to the current leakage at high voltage. The approximate energy output of the system was 0.25 mJ per cycle. Binh et al. [86] designed a floating wave energy converter that uses a control system, which aided in maximising the generated energy. The proposed control system allowed to increase the device efficiency of up to 25% in numerical simulations.

6.3. Vibro-impact harvester

Recently a novel DE-based device for EH from a vibrational motion has been proposed in [87, 88]. The main idea centres around a hollow cylinder, excited by an external force, and a free moving internal ball (friction was neglected), motion of which is constrained at both the ends of the cylinder by DE membranes. The ball motion is excited through its impacts against the DE membranes, which causes the membranes deformation (increase in the capacitance) leading to energy harvesting. The cylinder can be placed under an angle β with respect to the horizon. For an inclination angle $\beta = 0$ the motion of the cylinder should be large enough to engage the ball motion, however for any angle $\beta > 0$ the ball will be at rest on the lower membrane and its separation from the membrane will be engaged under a set of certain conditions. This design was called vibro-impacting EH and the dynamics of the generator has been investigated for various initial conditions, angles of inclination and restitution coefficients under deterministic and random loading. Numerically simulations have shown the rich nonlinear dynamics of the harvesters and indicated a mechanism for the device optimisation.

7. Conclusions

This chapter covers the fundamental aspects of Dielectric Elastomers and their potential application for Energy Harvesting. The chapter intended to overview the new developments made since the publication of [6]. There has been a significant progress made in understanding the material and electrical properties of DEs, optimisation of the energy harvesting process and modelling DEs. Some new ideas of ceasing the need for a substantial initial voltage using a self-priming circuit and ferroelectrics/electrets have been explored. New concepts of DE-based devices have been designed and tested. Nevertheless, it would be wrong to say that the behaviour of DEs and their capabilities have been entirely studied, thus more investigations are required.

Author details

Gordon Thomson[1]*, Daniil Yurchenko[1] and Dimitri V. Val[2]

*Address all correspondence to: grt2@hw.ac.uk

1 IMPEE, Heriot-Watt University, UK

2 EGIS, Heriot-Watt University, UK

References

[1] Pelrine R, Kornbluh R, Eckerle J, Jeuck P, Oh S, Pei Q, Stanford S. Dielectric elastomers: Generator mode fundamentals and applications. Proceedings of SPIE. 2001;**4329**:148-156

[2] Koh SJA, Zhao X, Suo Z. Maximal energy that can be converted by a dielectric elastomer generator. Applied Physics Letters. 2009;**94**(26)

[3] Mckay TG, Rosset S, Anderson IA, Shea H. Dielectric elastomer generators that stack up. Smart Materials and Structures. 2014;**24**(1)

[4] El-Hami M, Glynne-Jones P, White NM, Hill M, Beeby S, James E, Brown AD, Ross JN. Design and fabrication of a new vibration-based electromechanical power generator. Sensors and Actuators A: Physical. 2001;**92**(1):335-342

[5] Roundy S, Wright PK, Rabaey J. A study of low level vibrations as a power source for wireless sensor nodes. Computer Communications. 2003;**26**(11):1131-1144

[6] R Pelrine, H Prahlad. Generator Mode: Devices and Applications. Oxford: Elsevier. 2008

[7] Kornbluh RD, Pelrine R, Prahlad H, Wong-Foy A, McCoy B, Kim S, Eckerle J, Low T. From Boots to Buoys: Promises and Challenges of Dielectric Elastomer Energy Harvesting. Boston, MA: Springer US; 2012. pp. 67-93

[8] Miranda JOM. Electrostatic vibration-to-electric energy conversion [PhD thesis]. Massachusetts Institute of Technology; 2004

[9] Blokhina E, Galayko D, Basset P, Feely O. Steady-state oscillations in resonant electrostatic vibration energy harvesters. IEEE Transactions on Circuits and Systems I: Regular Papers. 2013;**60**(4):875-884

[10] Huang J, Shian S, Suo Z, Clarke DR. Maximizing the energy density of dielectric elastomer generators using equi-biaxial loading. Advanced Functional Materials. 2013;**23**(40): 5056-5061

[11] Shian S, Huang J, Zhu S, Clarke DR. Optimizing the electrical energy conversion cycle of dielectric elastomer generators. Advanced Materials. 2014;**26**(38):6617-6621

[12] Zhou J, Jiang L, Khayat RE. Analysis on the energy harvesting cycle of dielectric elastomer generators for performance improvement. EPL (Europhysics Letters). 2016;**115**(2)

[13] Hoffstadt T, Graf C, Maas J. Optimization of the energy harvesting control for dielectric elastomer generators. Smart Materials and Structures. 2013;**22**(9)

[14] Czech B, van Kessel R, Bauer P, Ferreira JA, Wattez A. Energy harvesting using dielectric elastomers. In: Power Electronics and Motion Control Conference (EPE/PEMC), 2010 14th International; IEEE; 2010. pp. S4-18

[15] Kornbluh R, Wong-Foy A, Ron Pelrine, Prahlad H, McCoy B. Long-lifetime all-polymer artificial muscle transducers. MRS Online Proceedings Library Archive. 2010 Jan; 1271

[16] Kaltseis R, Keplinger C, Baumgartner R, Kaltenbrunner M, Li T, Mächler P, Schwödiauer R, Suo Z, Bauer S. Method for measuring energy generation and efficiency of dielectric elastomer generators. Applied Physics Letters. 2011;**99**(16)

[17] Jean-Mistral C, Basrour S, Chaillout JJ. Comparison of electroactive polymers for energy scavenging applications. Smart Materials and Structures. 2010;**19**(8)

[18] Kornbluh RD, Pelrine R, Prahlad H, Wong-Foy A, McCoy B, Kim S, Eckerle J, Low T. Dielectric elastomers: Stretching the capabilities of energy harvesting. MRS Bulletin. 2012;**37**(3):246-253

[19] Biggs J, Danielmeier K, Hitzbleck J, Krause J, Kridl T, Nowak S, Orselli E, Quan X, Schapeler D, Sutherland W, et al. Electroactive polymers: Developments of and perspectives for dielectric elastomers. Angewandte Chemie International Edition. 2013;**52**(36): 9409-9421

[20] Romasanta LJ, Lopez-Manchado MA, Verdejo R. Increasing the performance of dielectric elastomer actuators: A review from the materials perspective. Progress in Polymer Science. 2015;**51**:188-211

[21] Madsen FB, Daugaard AE, Hvilsted S, Skov AL. The current state of silicone-based dielectric elastomer transducers. Macromolecular Rapid Communications. 2016;**37**(5):378-413

[22] Mockensturm EM, Goulbourne N. Dynamic response of dielectric elastomers. International Journal of Non-Linear Mechanics. 2006;**41**(3):388-395

[23] Schmidt A, Rothemund P, Mazza E. Multiaxial deformation and failure of acrylic elastomer membranes. Sensors and Actuators A: Physical. 2012;**174**:133-138

[24] Pharr M, Sun JY, Suo Z. Rupture of a highly stretchable acrylic dielectric elastomer. Journal of Applied Physics. 2012;**111**(10)

[25] Jiang L, Betts A, Kennedy D, Jerrams S. Investigation into the electromechanical properties of dielectric elastomers subjected to pre-stressing. Materials Science and Engineering: C. 2015;**49**:754-760

[26] Wissler M, Mazza E. Mechanical behavior of an acrylic elastomer used in dielectric elastomer actuators. Sensors and Actuators A: Physical. 2007;**134**(2):494-504

[27] Bernardi L, Hopf R, Ferrari A, Ehret AE, Mazza E. On the large strain deformation behavior of silicone-based elastomers for biomedical applications. Polymer Testing. 2017;**58**(Supplement C):189-198

[28] Kaltseis R, Keplinger C, Koh SJA, Baumgartner R, Goh YF, Ng WH, Kogler A, Tröls A, Foo CC, Suo Z, et al. Natural rubber for sustainable high-power electrical energy generation. RSC Advances. 2014;**4**(53):27905-27913

[29] Zhang J, Wang Y, Chen H, Li B. Energy harvesting performance of viscoelastic polyacrylic dielectric elastomers. International Journal of Smart and Nano Materials. 2015;**6**(3): 162-170

[30] Zhou J, Jiang L, Khayat RE. Methods to improve harvested energy and conversion efficiency of viscoelastic dielectric elastomer generators. Journal of Applied Physics. 2017;**121**(18)

[31] Wang H, Wang C, Yuan T. On the energy conversion and efficiency of a dielectric electro-active polymer generator. Applied Physics Letters. 2012;**101**(3)

[32] Hossain M, Vu DK, Steinmann P. Experimental study and numerical modelling of vhb 4910 polymer. Computational Materials Science. 2012;**59**:65-74

[33] Hossain M, Vu DK, Steinmann P. A comprehensive characterization of the electro-mechanically coupled properties of vhb 4910 polymer. Archive of Applied Mechanics. 2015;**85**(4):523-537

[34] Sahu R, Patra K, Szpunar J. Experimental study and numerical modelling of creep and stress relaxation of dielectric elastomers. Strain. 2015;**51**(1):43-54

[35] Helal A, Doumit M, Shaheen R. Biaxial experimental and analytical characterization of a dielectric elastomer. Applied Physics A. 2018;**124**(1):2

[36] Zhang R, Iravani P, Keogh P. Closed loop control of force operation in a novel self-sensing dielectric elastomer actuator. Sensors and Actuators A: Physical. 2017;**264**(Supplement C):123-132

[37] Foo CC, Cai S, Jin Adrian Koh S, Bauer S, Suo Z. Model of dissipative dielectric elastomers. Journal of Applied Physics. 2012;**111**(3)

[38] Diani J, Fayolle B, Gilormini P. A review on the Mullins effect. European Polymer Journal. 2009;**45**(3):601-612

[39] Carpi F, Anderson I, Bauer S, Frediani G, Gallone G, Gei M, Graaf C, Jean-Mistral C, Kaal W, Kofod G, et al. Standards for dielectric elastomer transducers. Smart Materials and Structures. 2015;**24**(10)

[40] Chen SE, Deng L, He ZC, Li E, Li GY. Temperature effect on the performance of a dissipative dielectric elastomer generator with failure modes. Smart Materials and Structures. 2016;**25**(5)

[41] Tröls A, Kogler A, Baumgartner R, Kaltseis R, Keplinger C, Schwödiauer R, Graz I, Bauer S. Stretch dependence of the electrical breakdown strength and dielectric constant of dielectric elastomers. Smart Materials and Structures. 2013;**22**(10)

[42] Yin G, Yang Y, Song F, Renard C, Dang ZM, Shi CY, Wang D. Dielectric elastomer generator with improved energy density and conversion efficiency based on polyurethane composites. ACS Applied Materials & Interfaces. 2017;**9**(6):5237-5243

[43] Graf C, Hitzbleck J, Feller T, Clauberg K, Wagner J, Krause J, Maas J. Dielectric elastomer–based energy harvesting: Material, generator design, and optimization. Journal of Intelligent Material Systems and Structures. 2014;**25**(8):951-966

[44] Suo Z. Theory of dielectric elastomers. Acta Mechanica Solida Sinica. 2010;**23**(6):549-578

[45] Carpi F, Gei M. Predictive stress–stretch models of elastomers up to the characteristic flex. Smart Materials and Structures. 2013;**22**(10)

[46] Graf C, Aust M, Maas J, Schapeler D. Simulation model for electro active polymer generators. In: Solid Dielectrics (ICSD) 2010 10th IEEE International Conference on 2010 Jul 4. IEEE; pp. 1-4

[47] Shiju E, Ge C, Cao J, Liu A, Jin L, Jiang X. Research on power generation of dielectric elastomer based on MATLAB. In: Mechatronics and Automation (ICMA), 2015 IEEE International Conference on 2015 Aug 2. IEEE; pp. 549-554

[48] Lv X, Liu L, Liu Y, Leng J. Dielectric elastomer energy harvesting: Maximal converted energy, viscoelastic dissipation and a wave power generator. Smart Materials and Structures. 2015;**24**(11)

[49] Wissler M, Mazza E. Modeling of a pre-strained circular actuator made of dielectric elastomers. Sensors and Actuators A: Physical. 2005;**120**(1):184-192

[50] Qu S, Suo Z. A finite element method for dielectric elastomer transducers. Acta Mechanica Solida Sinica. 2012;**25**(5):459-466

[51] Wissler M, Mazza E. Modeling and simulation of dielectric elastomer actuators. Smart Materials and Structures. 2005;**14**(6)

[52] Park HS, Suo Z, Zhou J, Klein PA. A dynamic finite element method for inhomogeneous deformation and electromechanical instability of dielectric elastomer transducers. International Journal of Solids and Structures. 2012;**49**(15):2187-2194

[53] Li T, Qu S, Yang W. Energy harvesting of dielectric elastomer generators concerning inhomogeneous fields and viscoelastic deformation. Journal of Applied Physics. 2012;**112**(3)

[54] Liu J, Foo CC, Zhang ZQ. A 3d multi-field element for simulating the electromechanical coupling behavior of dielectric elastomers. Acta Mechanica Solida Sinica. 2017;**30**(4):374-389

[55] Fox JW, Goulbourne NC. On the dynamic electromechanical loading of dielectric elastomer membranes. Journal of the Mechanics and Physics of Solids. 2008;**56**(8):2669-2686

[56] Steinmann P, Hossain M, Possart G. Hyperelastic models for rubber-like materials: Consistent tangent operators and suitability for Treloar's data. Archive of Applied Mechanics. 2012;**82**(9):1183-1217

[57] Hossain M, Steinmann P. More hyperelastic models for rubber-like materials: Consistent tangent operators and comparative study. Journal of the Mechanical Behavior of Materials. 2013;**22**(1–2):27-50

[58] Wang Y, Chen H, Wang Y, Li D. A general visco-hyperelastic model for dielectric elastomers and its efficient simulation based on complex frequency representation. International Journal of Applied Mechanics. 2015;**7**(01)

[59] Zhang J, Chen H. Electromechanical performance of a viscoelastic dielectric elastomer balloon. International Journal of Smart and Nano Materials. 2014;**5**(2):76-85

[60] Kollosche M, Kofod G, Suo Z, Zhu J. Temporal evolution and instability in a viscoelastic dielectric elastomer. Journal of the Mechanics and Physics of Solids. 2015;**76**:47-64

[61] Chang M, Wang Z, Tong L, Liang W. Effect of geometric size on mechanical properties of dielectric elastomers based on an improved visco-hyperelastic film model. Smart Materials and Structures. 2017;**26**(3)

[62] Zhang J, Ru J, Chen H, Li D, Lu J. Viscoelastic creep and relaxation of dielectric elastomers characterized by a Kelvin-Voigt-Maxwell model. Applied Physics Letters. 2017;**110**(4)

[63] Hong W. Modeling viscoelastic dielectrics. Journal of the Mechanics and Physics of Solids. 2011;**59**(3):637-650

[64] Bortot E, Denzer R, Menzel A, Gei M. Analysis of viscoelastic soft dielectric elastomer generators operating in an electrical circuit. International Journal of Solids and Structures. 2016;**78**:205-215

[65] Wineman A. Nonlinear viscoelastic solids—A review. Mathematics and Mechanics of Solids. 2009;**14**(3):300-366

[66] O'Brien B, McKay TG, Calius E, Xie S, Anderson I. Finite element modelling of dielectric elastomer minimum energy structures. Applied Physics A: Materials Science & Processing. 2009;**94**(3):507-514

[67] Henann DL, Shawn AC, Bertoldi K. Modeling of dielectric elastomers: Design of actuators and energy harvesting devices. Journal of the Mechanics and Physics of Solids. 2013;**61**(10):2047-2066

[68] Cohen N, Menzel A, et al. Towards a physics-based multiscale modelling of the electro-mechanical coupling in electro-active polymers. In: Proceedings of the Royal Society of London. 2016 Feb 1;**472**(2186):20150462

[69] Jean-Mistral C, Vu Cong T, Sylvestre A. Advances for dielectric elastomer generators: Replacement of high voltage supply by electret. Applied Physics Letters. 2012;**101**(16)

[70] O'Dwyer JJ. The Theory of Electrical Conduction and Breakdown in Solid Dielectrics. Clarendon Press; 1973

[71] Kofod G, Sommer-Larsen P, Kornbluh R, Pelrine R. Actuation response of polyacrylate dielectric elastomers. Journal of Intelligent Material Systems and Structures. 2003;**14**(12):787-793

[72] Pelrine R, Kornbluh R. Dielectric elastomers as electroactive polymers (eaps): Fundamentals. In: Capri F, editor. Electromechanically Active Polymers. Switzerland: Springer International Publishing; 2016; p. 671

[73] Zhou J, Jiang L, Khayat RE. Investigation on the performance of a viscoelastic dielectric elastomer membrane generator. Soft Matter. 2015;**11**(15):2983-2992

[74] Rudykh S, Bhattacharya K, et al. Multiscale instabilities in soft heterogeneous dielectric elastomers. In: Proceedings of the Royal Society of London A. 2014 Feb 8;**470**(2162)

[75] Zhang R, Huang X, Li T, Iravani P, Keogh P. Novel arrangements for high performance and durable dielectric elastomer actuation. Actuators. 2016;**5**(3)

[76] McKay TG, O'Brien B, Calius E, Anderson I. Self-priming dielectric elastomer generators. Smart Materials and Structures. 2010;**19**(5)

[77] Illenberger P, Takagi K, Kojima H, Madawala UK, Anderson IA. A mathematical model for self-priming circuits: Getting the most from a dielectric elastomer generator. IEEE Transactions on Power Electronics. 2017;**32**(9):6904-6912

[78] Panigrahi R, Mishra SK. An electrical model of a dielectric elastomer generator. IEEE Transactions on Power Electronics. 2018 Apr;**33**(4):2792-2797

[79] Jean-Mistral C, Porter T, Vu-Cong T, Chesne S, Sylvestre A. Modelling of soft generator combining electret and dielectric elastomer. In: 2014 IEEE/ASME International Conference on Advanced Intelligent Mechatronics (AIM). IEEE; 2014. pp. 1430-1435

[80] Huang J, Shian S, Suo Z, Clarke DR. Dielectric elastomer generator with equi-biaxial mechanical loading for energy harvesting. In: Electroactive Polymer Actuators and Devices (EAPAD). International Society for Optics and Photonics. 2013 Apr 9;**8687**: 86870Q

[81] McKay TG, Rosset S, Anderson IA, Shea H. An electroactive polymer energy harvester for wireless sensor networks. In: Journal of Physics: Conference Series. Vol. 476, No. 1. IOP Publishing; 2013

[82] Lai H, Tan CA, Xu Y. Dielectric elastomer energy harvesting and its application to human walking. In: ASME 2011 International Mechanical Engineering Congress and Exposition. American Society of Mechanical Engineers. 2011 Jan 1; pp. 601-607

[83] Moretti G, Fontana M, Vertechy R. Model-based design and optimization of a dielectric elastomer power take-off for oscillating wave surge energy converters. Meccanica. 2015; **50**(11):2797-2813

[84] Moretti G, Righi M, Vertechy R, Fontana M. Fabrication and test of an inflated circular diaphragm dielectric elastomer generator based on pdms rubber composite. Polymer. 2017;**9**(7):283

[85] Vertechy R, Fontana M, Papini GPR, Forehand D. In-tank tests of a dielectric elastomer generator for wave energy harvesting. In: Electroactive Polymer Actuators and Devices (EAPAD) 2014. Vol. 9056. International Society for Optics and Photonics; 2014

[86] Binh PC, Ahn KK. Performance optimization of dielectric electro active polymers in wave energy converter application. International Journal of Precision Engineering and Manufacturing. 2016;**17**(9):1175-1185

[87] Yurchenko D, Val DV, Lai ZH, Gu G, Thomson G. Energy harvesting from a de-based dynamic vibro-impact system. Smart Materials and Structures. 2017;**26**(10)

[88] Yurchenko D, Lai ZH, Thomson G, Val DV, Bobryk RV. Parametric study of a novel vibro-impact energy harvesting system with dielectric elastomer. Applied Energy. 2017;**208**:456-470